



http://pubs.acs.org/journal/acsodf Article

Colorimetric Detection of Dopamine with J-Aggregate Nanotube-Integrated Hydrogel Thin Films

Nitin Ramesh Reddy, Samuel Rhodes, and Jiyu Fang*



Cite This: ACS Omega 2020, 5, 18198-18204



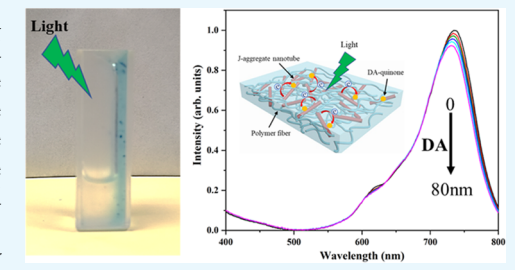
ACCESS

Metrics & More

Article Recommendations

Supporting Information

ABSTRACT: The deficiency of dopamine (DA) is clinically linked to several neurological diseases. The detection of urinary DA provides a noninvasive method for diagnosing these diseases and monitoring therapies. In this paper, we report the coassembly of lithocholic acid (LCA) and 3,3'-diethythiadicarbocyanine iodide (DiSC $_2(5)$) at the equimolar ratio in ammonia solution into J-aggregate nanotubes. By integrating the J-aggregate nanotubes into transparent agarose hydrogel films formed on the wall of quartz cuvettes, we fabricate a portable and reproducible sensor platform for the optical detection of DA in synthetic urine. The J-band intensity of the integrated J-aggregate nanotubes is found to linearly decrease with the increase of DA concentrations from 10 to 80 nM, giving the limit



of detection of \sim 7 nM. The detection mechanism is based on the photoinduced electron transfer (PET) from the excited J-aggregate nanotubes to adsorbed DA-quinone. The PET process used in the sensor platform can reduce the interference of ascorbic acid and uric acid in the detection of DA in synthetic urine. The high sensitivity of the sensor platform is contributed by the delocalized exciton of J-aggregate nanotubes.

■ INTRODUCTION

Dopamine (DA) is a neurotransmitter, which is critical for the function of central nervous systems such as movement, memory, and reward regulations. The deficiency of DA has been implicated in nervous system diseases. Due to the importance of DA in central nervous systems, there has been great interest in developing sensitive methods to detect DA in vivo/in vitro with the goal of diagnosing nervous system diseases or monitoring therapies. Electrochemical analysis, 2-6 enzyme-linked immunosorbent assay, 7,8 electrophoresis, 9 and chromatography¹⁰ are commonly used for the detection of DA in biological fluids. However, these analytical methods need expensive enzymes, multistep reactions, and specialized instruments. Recently, colorimetric sensors based on inorganic nanoparticles have been developed for the sensitive and selective detection of DA in an aqueous solution and biological fluids. 11-15 The advantage of the colorimetric sensors includes low cost, rapid detection, and high sensitivity.

Photoinduced electron transfer (PET) is a common approach in the synthesis of colorimetric and fluorometric probes. Thus, a possible method of improving the performance of optical sensors is to design highly efficient PET probes. J-aggregates represent an ordered structure formed by the head-to-tail staircase arrangement of dyes. The strong interaction of transition dipole moments in J-aggregates can lead to the formation of new electronic excitations. The delocalized excitation of J-aggregates favors highly efficient PET processes. Due to the remarkable optical and transport properties, J-aggregates have shown promise as an optical probe in bioimaging 21–23 and biosensing. Pre-

viously, we showed that J-aggregate nanotubes from the coassembly of lithocholic acid (LCA) and 3,3'-dipropylth-iadicarbocyanine iodide (DiSC $_3(5)$) with an equimolar ratio could serve as an efficient PET supramolecular probe for the sensitive and selective detection of DA in a PBS solution in the presence of ascorbic acid (AA) and uric acid (UA). ²⁶

However, one of the challenges of using J-aggregate nanotubes as optical probes for the detection of biological species in biological fluids is their diffusion and sedimentation over time, which may lead to a discrepancy in the detection. Polymer hydrogels are a three-dimensional cross-linked network system, which is able to immobilize colloid particles, but permeable for small molecules. In this paper, we formed J-aggregate nanotubes by the coassembly of lithocholic acid (LCA) and 3,3'-diethythiadicarbocyanine iodide (DiSC₂(5)) at the equimolar ratio in ammonia solution and then integrated them into transparent agarose hydrogel films, forming a simple and portable sensor platform for the optical detection of DA in synthetic urine, in which the features of both agarose hydrogels and J-aggregate nanotubes were synergized (Figure 1).

Received: April 19, 2020 Accepted: July 3, 2020 Published: July 17, 2020





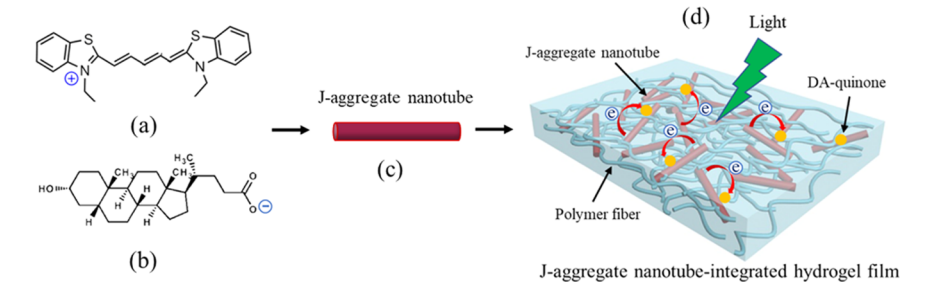


Figure 1. Chemical structure of 3,3'-diethylthiadicarbocyanine iodide (DiSC₂(5)) (a) and lithocholic acid (LCA) (b). Schematic illustration of Jaggregate nanotubes (c) and J-aggregate nanotube-integrated agarose hydrogel films with the photoinduced electron transfer from the J-aggregate nanotubes to adsorbed dopamine (d).

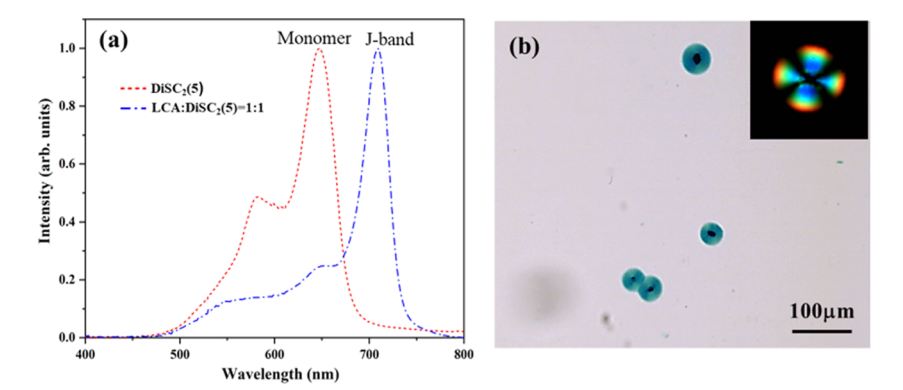


Figure 2. (a) Adsorption spectrum of the LCA/DiSC₂(5) solution formed by dissolving 1 mM LCA and 1 mM DiSC₂(5) in 1% ammonia solution, together with the adsorption spectrum of 1 mM DiSC₂(5) in methanol. (b) Optical microscopy image of coassembled J-aggregate spherulites in 1% ammonia solution. Polarizing optical microscopy image of a J-aggregate spherulite is inserted in (b).

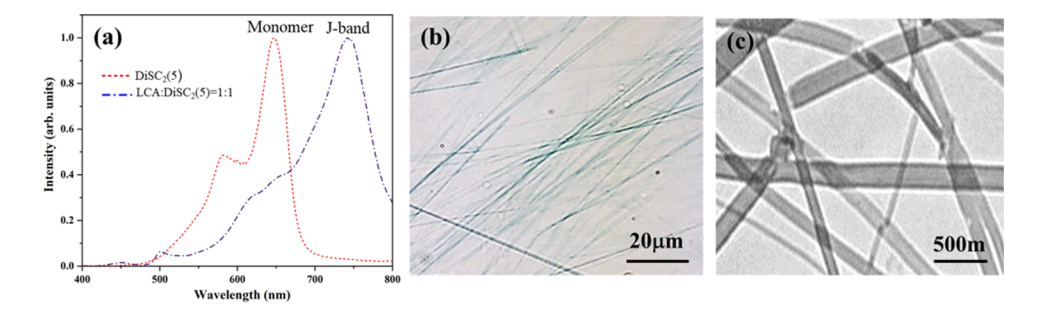


Figure 3. (a) Adsorption spectrum of the LCA/DiSC₂(5) solution formed by dissolving 1 mM LCA and 1 mM DiSC₂(5) in 30% ammonia solution, together with the adsorption spectrum of 1 mM DiSC₂(5) in methanol. (b) Optical microscopy and (c) TEM images of coassembled Jaggregate nanotubes formed at the mixed LCA/DiSC₂(5) molar ratio of 1:1 in 30% ammonia solution.

■ RESULTS AND DISCUSSION

Preparation and Characterization of J-Aggregate **Nanotubes.** The structures of $DiSC_2(5)$ and LCA are shown in Figure 1a,b, respectively. LCA contains a steroid backbone and a carboxyl group linked to the steroid backbone with a short alkyl chain. The critical micelle concentration (CMC) of LCA in an aqueous solution is ~0.9 mM.²⁸ $DiSC_2(5)$ consists of two nitrogen centers, one of which is positively charged. They are linked by a polymethine chain. DiSC₂(5) monomers in methanol showed an absorption band at 647 nm (Figure 2a). In the presence of 1 mM LCA, 1 mM DiSC₂(5) formed J-aggregates with a J-band at 711 nm in 1% ammonia solution. The J-band was shifted by 64 nm with respect to the monomer band of DiSC₂(5). The J-aggregates from the coassembly of DiSC₂(5) and LCA at the equimolar ratio showed a spherulitic morphology (Figure 2b). The presence of DiSC₂(5) in the fibers surrounding the core of the

spherulite was evident from the blue color. Under a polarizing optical microscopy, the Maltese-cross extinction pattern of spherulitic J-aggregates was observed (see the inset in Figure 2b), suggesting the ordering of the J-aggregate fibers. The spherulitic J-aggregates were unstable and easily broken by brief sonication (Figure S1a).

The solubility of cyanine dyes in ammonia solution can be increased by increasing ammonia concentrations. ²⁹ In 30% ammonia solution, 1 mM $\mathrm{DiSC}_2(5)$ formed J-aggregates with a relatively broad absorbance with the maximum at 740 nm in the presence of 1 mM LCA (Figure 3a). The J-aggregates showed a tubular morphology with blue color (Figure 3b). The hollowness of the J-aggregate nanotubes was evident in the transmission electron microscopy (TEM) image shown in Figure 3c. It was also clear in the TEM image that the J-aggregate nanotubes were polydisperse with the diameters from 80 to 240 nm, which were much larger than that formed

from the coassembly of LCA and DiSC₃(5) with an equimolar ratio in the NaOH aqueous solution. The pK_a value of LCA in the aqueous solution is ~7.0. In 30% ammonia solution with pH 13, LCA was ionized. Ionized LCA could self-assemble into nanotubes in ammonia solution.³⁰ It was reported that hydrophobic molecules could be capsulated in the hydrophobic cavity of bile acid micelles.³¹ In our experiments, the concentration of LCA was higher than its CMC. Thus, we could assume that DiSC₂(5) molecules were first capsulated in LCA micelles through the coassembly. The mixed micelles then assembled into nanotubes, in which DiSC₂(5) formed Jaggregates in the wall of the nanotubes. To verify the assumption, we studied the aggregation behavior of 1 mM DiSC₂(5) in the presence of 0.5 mM LCA in 30% ammonia solution, in which the concentration of LCA was lower than its CMC. In this case, DiSC₂(5) formed H-aggregates with the Hband at 448 nm (Figure S2), which agrees with the H-band of H-aggregates of DiSC₂(5) formed in 30% ammonia solution without the presence of LCA. This result suggests that LCA is unable to serve as a direct agent when its concentration is lower than CMC. We noted that J-aggregates could be formed by the coassembly of 1 mM LCA and 0.2 mM DiSC₂(5) in 30% ammonia solution (Figure S3a). The absorbance of the Jaggregate from the coassembly of 1 mM LCA and 0.2 mM $DiSC_2(5)$ was slightly wider than that from the coassembly of 1 mM LCA and 1 mM DiSC₂(5). Blue color J-aggregate nanotubes were visible in the optical microscopy image shown in Figure S3b. The diameter of J-aggregate nanotubes was in the range from 120 to 550 nm (Figure S3c). Partially broken Jaggregate nanotubes were occasionally observed (Figure S3d), which confirmed their hollowness.

Fabrication of J-Aggregate Nanotube-Integrated Hydrogel Films. Agarose was reported to form transparent and neutral hydrogels in the aqueous solution through hydrogen bonding.³² The pore size of agarose hydrogels was found in the range from 50 to 100 nm. 33 Using a horizontally placed quartz cuvette as a mold, we formed a J-aggregate nanotube-integrated hydrogel film on the wall of the cuvette. The hydrogel film was able to adhere on the wall of the quartz cuvette even after the addition of synthetic urine (Figure 4a), providing a simple and portable sensor platform, in which the sedimentation of J-aggregate nanotubes was limited by the hydrogel network, but DA could diffuse into the hydrogel film and reach to the J-aggregate nanotubes. The J-aggregate nanotube-integrated hydrogel film could also be taken out from the quartz cuvette (Figure 4b). The blue color Jaggregate nanotubes integrated into the hydrogel films were clearly visible in the optical microscopy image shown in Figure 4c. They showed the expected shape and size distributions. The viscoelastic properties of agarose hydrogel films with/ without J-aggregate nanotubes were characterized. The storage modulus (G') of J-aggregate nanotube-integrated hydrogel films was about 10 times higher than their loss modulus (G'')(Figure 4d). It is also clear in Figure 4d that the G' of agarose hydrogel films with J-aggregate nanotubes was higher than that of pure agarose hydrogel films, suggesting that the integration of J-aggregate nanotubes restrained the movement of agarose chains in the hydrogel network.

Sensitivity for Dopamine Detection. The analysis of urinary DA is a noninvasive method for diagnosing nervous system diseases and evaluating the effectiveness of treatments.³⁴ Synthetic urine is often used to mimic the characteristics of urine. In our experiments, 1 mL of diluted

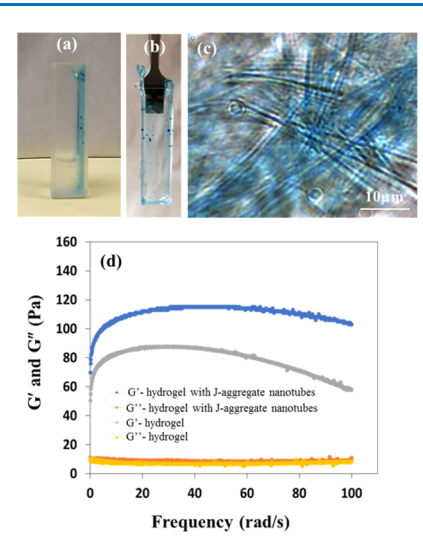
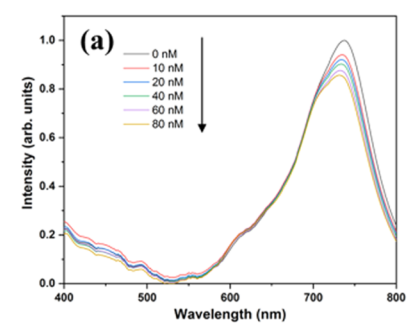
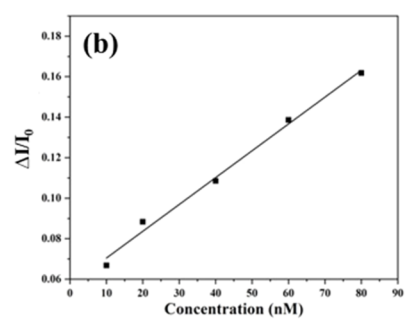


Figure 4. Photography images of J-aggregate nanotube-integrated agarose hydrogel films before (a) and after (b) being taken out from a quartz cuvette. (c) Optical microscopy image of J-aggregate nanotube-integrated agarose hydrogel films. (d) Frequency sweeps of agarose hydrogel films with and without J-aggregate nanotubes formed at the mixed LCA/DiSC₂(5) molar ratio of 1:1.

synthetic urine (100 times) was added into the cuvette with the J-aggregate nanotube-integrated hydrogel film (Figure 4a). We noted that the J-aggregate nanotubes integrated into the agarose hydrogel film were stable in synthetic urine and showed no change in their absorbance over time (Figure S4a). In addition, the J-band position of the J-aggregate nanotubes integrated into agarose hydrogel films was the same as that of the J-aggregate nanotubes formed in ammonia solution, suggesting that the gelation process did not disrupt the packing of DiSC₂(5) in the nanotubes. The J-aggregate nanotubes integrated into hydrogel films in synthetic urine were also photostable (Figure S4b). Synthetic urine used in our experiments contains urea, sodium chloride, magnesium sulfate heptahydrate, and calcium chloride dehydrate. The stability shown in Figure S4 suggests that the integrated Jaggregate nanotubes are insensitive to these chemicals in synthetic urine. We would like to point out that the absorbance of J-aggregate spherulites integrated into agarose hydrogel films decreased in synthetic urine over time (Figure S1b). Jaggregate spherulites easily broke up into small J-aggregate fibers and fanlike J-aggregates by sonication (Figure S1a). The agarose hydrogel network was unable to immobilize small Jaggregate fibers and fanlike J-aggregates. After the addition of synthetic urine, we noted that these small J-aggregates gradually precipitated in the hydrogel film. Therefore, we only exploited the potential of J-aggregate nanotube-integrated hydrogel films for the detection of DA in synthetic urine. In our experiments, DA with different concentrations was added into the synthetic urine in the cuvette with the J-aggregate nanotube-integrated hydrogel film in the dark. After 10 min incubation, which allowed DA to diffuse into the hydrogel film and adsorb at the surface of the integrated J-aggregate nanotubes, we irradiated the integrated J-aggregate nanotube with a flashlight for 30 s, followed by measuring their adsorption spectra. The J-band intensity of the integrated Jaggregate nanotubes decreased with the increase of DA concentrations from 10 to 80 nM in synthetic urine (Figure 5a), where J-aggregate nanotubes were formed at the mixed





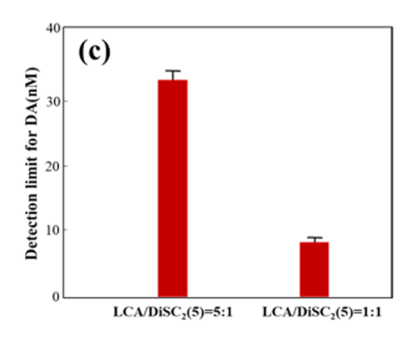
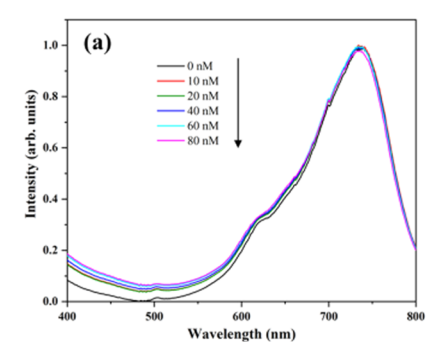
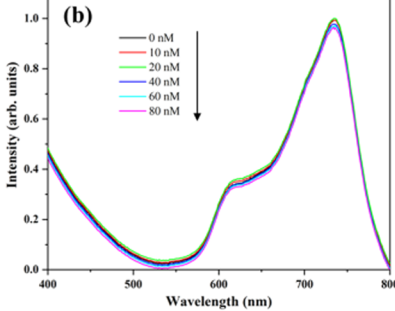


Figure 5. (a) Absorption spectra of J-aggregate nanotube-integrated agarose hydrogel films in synthetic urine with 0, 10, 20, 40, 60, and 80 nM DA. J-aggregate nanotubes were formed at the mixed molar ratio of 1:1. (b) Plot of $\Delta I/I_0$ as a function of DA concentrations in synthetic urine. (c) Detection limit of J-aggregate nanotube-integrated hydrogel films for DA in synthetic urine. J-aggregate nanotubes were formed at the mixed LCA/DiSC₂(5) molar ratio of 1:1 and 5:1, respectively. Results shown in (c) were the average value from three tests.





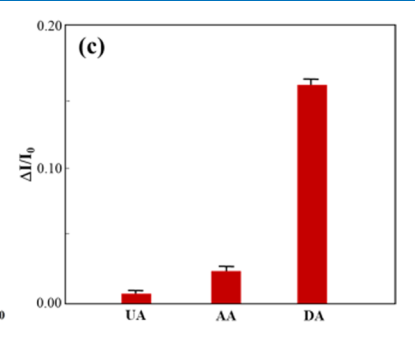


Figure 6. Absorption spectra of J-aggregate nanotube-integrated agarose hydrogel films in synthetic urine with 0, 10, 20, 40, 60, and 80 nM UA (a) and AA (b). J-aggregate nanotubes were formed at the mixed $LCA/DiSC_2(5)$ molar ratio of 1:1. (c) Relative J-band intensity changes in J-aggregate nanotubes integrated agarose hydrogel films upon addition of 80 nM UA, 80 nM AA, and 80 nM DA in synthetic urine, respectively. Results shown in (c) were the average value from three tests.

 $LCA/DiSC_2(5)$ molar ratio of 1:1. Figure 5b shows the plot of the relative intensity change $(\Delta I/I_0)$ in the J-band as a function of DA concentrations in synthetic urine, which showed a linear relationship. Here, $\Delta I = I_0 - I$, I_0 is the J-band intensity before the addition of DA, and I is the J-band intensity after the addition of DA. The detection limit for DA was estimated by multiplying the ratio of the standard deviation to the slope of the linear fit curve by 3.3, as shown in Figure 5b. The multiple detection tests using three J-aggregate nanotube-integrated hydrogel films made at the same conditions gave an average detection limit of 7.0 ± 0.3 nM for DA (Figure 5c). The detection limit for DA is 1 order of magnitude lower than that of these analytical methods reported in the literature²⁻⁵ and comparable to those of the colorimetric methods based on the plasmon absorption of nanoparticles. 11-13 It is known that the sedimentation of nanoparticles may occur in a solution, which can cause a discrepancy in the optical detection of DA. For the sensor platform reported here, agarose hydrogel networks immobilize J-aggregate nanotubes and reduce the discrepancy in the detection of DA in biological fluids.

For J-aggregate nanotubes formed at the mixed LCA/DiSC₂(5) molar ratio of 5:1 (1 mM LCA and 0.2 mM DiSC₂(5)), the absorbance decrease was also observed as the concentration of DA increased from 10 to 80 nM (Figure S5a). The plot of the relative intensity ($\Delta I/I_0$) of the J-band as a function of DA concentrations revealed a linear relationship (Figure S5b). The multiple measurements showed the average detection limit of 32.0 \pm 0.5 nM for DA (Figure 5c), which was higher than that of the J-aggregate nanotubes formed at the mixed LCA/DiSC₂(5) molar ratio of 1:1. The sensitivity of

J-aggregate nanotubes for DA depends on their delocalized excitation lengths, e.g., the number of coherently coupled $\mathrm{DiSC}_2(5)$ molecules in the J-aggregate nanotubes. The delocalized excitation of J-aggregates relates to the sharpness of their absorbances. As can be seen in Figures 5a and S5a, the full width at half-maximum (FWHM) of the adsorption spectrum of J-aggregate nanotubes formed at the mixed LCA/ $\mathrm{DiSC}_2(5)$ molar ratio of 1:1 is ~90 nm, which is smaller than that at the mixed LCA/ $\mathrm{DiSC}_2(5)$ molar ratio 5:1 (110 nm). Thus, we concluded that the number of coherently coupled $\mathrm{DiSC}_2(5)$ molecules in the J-aggregate nanotubes formed at the mixed ratio of 1:1 was higher than that at the mixed ratio of 5:1, giving a lower detection limit for DA.

Selectivity for Dopamine Detection. The interference from ascorbic acid (AA) and uric acid (UA) (Figure S6), which often coexist with DA in biological fluids, ³⁶ is the major challenge in the detection of DA. UA and urea are major components in urine. Our control experiments showed that the intensity of the J-band on the integrated J-aggregate nanotubes is insensitive to urea in synthetic urine (Figure S4). Thus, we further examined the selectivity of J-aggregate nanotubeintegrated hydrogel films by monitoring their optical response to AA and UA, respectively. In the selectivity examination, AA or UA at concentrations of 10, 20, 40, 60, and 80 nM were added in synthetic urine. After 10 min incubation in each case, we irradiated the J-aggregate nanotube-integrated hydrogel films with a flashlight for 30 s, followed by measuring their adsorption spectra (Figure 6a,b). The reduction of the relative J-band intensity by 80 nM UA and 80 nM AA was significantly smaller than that by 80 nM DA (Figure 6c). The result confirms the feasibility of J-aggregate nanotube-integrated hydrogel films as a colorimetric probe for the selective detection of DA in the presence of UA and AA.

Mechanism of DA Detection. It was reported that the autoxidation of DA occurred in an aqueous solution with a pH higher than 7.0, leading to the formation of the quinone form (Figure 7a). 36,37 The p K_a value of DA-quinone was 9.58. 38

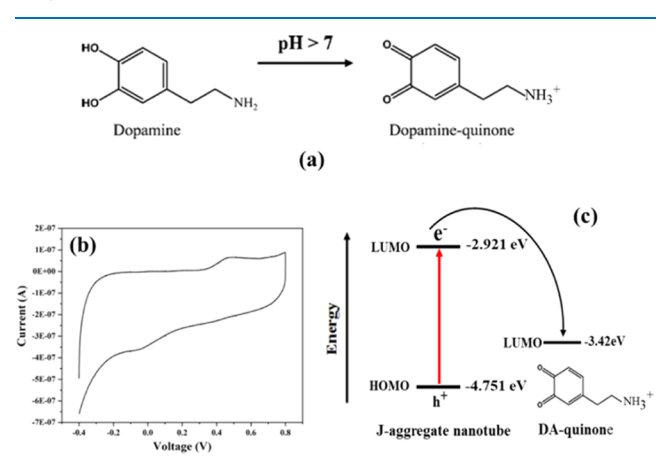


Figure 7. (a) Schematic illustration of the oxidization of DA in an aqueous solution. (b) Cyclic voltammogram of J-aggregate nanotubes formed at the mixed LCA/DiSC₂(5) molar ratio of 1:1. (c) Schematic energy band diagram of J-aggregate nanotubes and DA-quinone.

Thus, DA should exist as the quinone form and be positively charged in synthetic urine with pH 7.8-8.0. The positively charged DA-quinone diffused into hydrogel films and adsorbed on the surface of the integrated J-aggregate nanotubes through the electrostatic interaction with negatively charged LCA. DAquinone showed the absorbance with the peak at \sim 280 nm, ¹⁸ while the J-band of J-aggregate nanotubes was at \sim 740 nm. Thus, the Förster resonance energy transfer from the Jaggregate nanotubes to the adsorbed DA-quinone unlikely occurs. Whether or not the electron transfer from a donor to an acceptor occurs depends on the relative position of its highest occupied molecular orbital (HOMO) and the lowest unoccupied molecular orbital (LUMO) levels. DA-quinone has the HOMO level of -6.01 eV and the LUMO level of -3.42eV, respectively.³⁹ To estimate the HOMO and LUMO levels of J-aggregate nanotubes formed at the mixed molar ratio of 1:1, we measured their oxidation and reduction potentials with cyclic voltammetry (CV). As can be seen in the CV curve shown in Figure 7b, the J-aggregate nanotubes showed an oxidation peak. Thus, we calculated the HOMO and LUMO levels of J-aggregate nanotubes from the following equations⁴⁰

$$E(HOMO) = -e(E_{onset} + 4.4)$$
 (1)

$$E(LUMO) = E_g - E(HOMO)$$
 (2)

The onset oxidation peak $(E_{\rm onset})$ in the CV curve was 0.351 eV. The HOMO level calculated from eq 1 was -4.751 eV. $E_{\rm g}$ shown in eq 2 is the optical band gap energy that can be calculated according to the equation $E_{\rm g}=1242/\lambda_{\rm onset}$. For the J-aggregate nanotubes, $\lambda_{\rm onset}$ was $\sim\!678$ nm. Thus, $E_{\rm g}$ was calculated to be 1.83 eV. Based on eq 2, the LUMO level of the J-aggregate nanotubes was found to be -2.921 eV. It is clear that the LUMO level of DA-quinone is inside the HOMO–LUMO energy gap of the J-aggregate nanotubes (Figure 7c), meeting the requirement of the PET process from the excited

J-aggregate nanotubes to the adsorbed DA-quinone. Under light irradiation, electrons are excited from the ground state to the excited state of J-aggregate nanotubes. The DA-quinone absorbed at the surface of the J-aggregate nanotubes accepts the excited electrons (Figure 7c). Due to the delocalized excitation of J-aggregate nanotubes, the excited electrons can efficiently transfer to the adsorbed DA-quinone, giving the good sensitivity of J-aggregate nanotube-integrated hydrogel films in the detection of DA in synthetic urine.

The selectivity of J-aggregate nanotube-integrated hydrogel films for DA over UA and AA in synthetic urine can also be explained by the PET process. UA and AA could not be oxidized in an aqueous solution with pH higher than 7.0.⁴¹ Thus, they cannot serve as a good electron acceptor in synthetic urine with pH in the range of 7.8–8.0, and the PET process is not effective. To further verify the detection mechanism for DA, we measured the relative J-band intensity change in the J-aggregate nanotubes integrated into hydrogel films in a buffer solution with pH 7.0 and 10.0 after the addition of 80 nM DA. As can be seen in Figure 8, the J-band

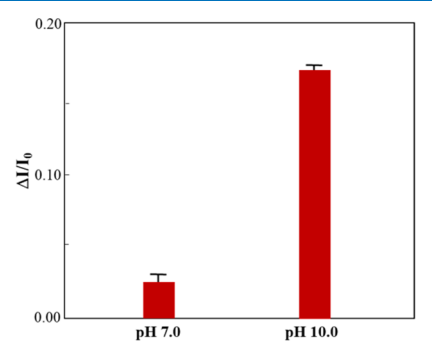


Figure 8. Relative J-band intensity change in the J-aggregate nanotubes integrated agarose hydrogel films in a buffer solution with pH 7.0 and 10.0 upon the addition of 80 nM DA. J-aggregate nanotubes were formed at the mixed LCA/DiSC $_2(5)$ molar ratio of 1:1. Results were the average value from three tests.

intensity change was significantly low at pH 7.0, compared to that in pH 10.0. This is because the number of DA molecules oxidized was low at pH 7.0. This result further confirms that PET is responsive to the detection of DA in synthetic urine.

CONCLUSIONS

We report the formation of J-aggregate nanotubes by the coassembly of LCA and DiSC₂(5) in ammonia solution. By integrating the J-aggregate nanotubes in agarose hydrogel films formed on the wall of quartz cuvettes, we fabricate a sensor platform for the optical detection of DA in synthetic urine, which combines the advantages of both agarose hydrogels and J-aggregate nanotubes. In the presence of DA in synthetic urine, the J-band intensity of the immobilized J-aggregate nanotubes decreases linearly with the increase of DA concentrations from 10 to 80 nM, giving the detection limit as low as ~7 nM. Furthermore, we find that J-aggregate nanotubes are less sensitive to UA and AA, compared to DA. The optical response of J-aggregate nanotube-integrated hydrogel films is a result of PET from the excited J-aggregate nanotubes to the adsorbed DA-quinone. Benefiting from the delocalized excitation of J-aggregates and the PET mechanism, the optical sensor shows high sensitivity to DA over UA and AA. We believe that the simple, low cost, portable, and reliable platform will open a new avenue for the fabrication of nanoparticle-based optical sensors as well.

■ EXPERIMENTAL SECTION

Materials. Lithocholic acid (LCA), 3,3'-diethylthiadicarbocyanine iodide (DiSC₂(5)), agarose, dopamine (DA), ascorbic acid (AA), and uric acid (UA) were purchased from Sigma-Aldrich and used as received. Ammonia solution was from Sigma-Aldrich. De-ionized (DI) water was obtained from Easypure II system (18 M Ω cm, pH 5.7). Synthetic urine with pH 7.8–8.0 was from Ricca Chemical Company and diluted 10 times with DI water before being used. Holey Formvar filmed grids were purchased from Electron Microscopy Science.

Synthesis and Characterization of J-Aggregate Nanotubes. The coassembly of LCA and DiSC₂(5) with the mixed molar ratio of 1:1 and 5:1 was carried out in 1 and 30% ammonia solution, in which the concentration of LCA was always kept at 1 mM. The mixture was sonicated in an ultrasonic bath (Branson 1510, Branson Ultrasonics Co.) for 5 min and then allowed to sit in the dark at room temperature for 24 h. The structure and morphology of coassembled Jaggregate nanotubes were characterized with an optical microscope (Olympus BX), a scanning electron microscope (SEM, Hitachi S3500N), and a transmission electron microscope (TEM, FEW Technai F30). For optical microscope observations, a drop of the mixed LCA/DiSC₂(5) solution was placed on a glass substrate, followed by placing a cover glass slide on the top of the drop. For SEM and TEM measurements, J-aggregate nanotubes were dried on holey Formvar filmed grids at room temperature for 24 h and then imaged at an accelerating voltage of 20 and 100 kV, respectively. The absorption spectra of the coassembled Jaggregate nanotubes were taken with a Cary 60 UV-vis spectrophotometer. Cyclic voltammetry (CV) measurements were conducted in an aqueous solution with 1 M KCl using CHI627C Electrochemical workstation, in which the coassembled J-aggregate nanotubes were placed on an ITO working electrode, a platinum wire severed as the counter electrode, and Ag/AgCl acted as a reference electrode. The scan range varied from -0.4 to 0.8 V at the speed of 0.01 V/s.

Fabrication of J-Aggregate Nanotube-Integrated Hydrogel Films. In total, 1 wt % agarose solution was formed by dissolving 0.1 g of agarose powder in 10 mL of 1% ammonia solution at ~40 °C under magnetic stirring. Our primary study showed that agarose could not form transparent hydrogels in 30% ammonia solution. Thus, ammonia was allowed to evaporate from the J-aggregate nanotube solution for 24 h at room temperature. Typically, 2.5 mL of J-aggregate solution after 24 h evaporation was then mixed with 2.5 mL of agarose solution. The mixed solution was stirred for 2 min and then transferred onto a horizontally placed quartz cuvette on a table. The gelation of the mixed solution in the cuvette occurred when the temperature was reduced to 23 °C, leading to the formation of a J-aggregate nanotube-integrated agarose hydrogel film on the wall of a quartz cuvette. Although the number of J-aggregate nanotubes integrated into agarose films was unknown, the total number of J-aggregate nanotubes was expected to be the same in agarose hydrogel films formed at the same conditions. The J-aggregate nanotube-integrated hydrogel films were taken out from the cuvette and then characterized using a rotational rheometer (AR 2000 ex, TA Instruments). The amplitude sweep was first performed at a

frequency of 1 Hz to check the linear viscoelastic region in the oscillation mode. Frequency sweeps were then carried out under the oscillation mode at 1% strain from 0.1 to 100 rad/s.

Detection of Dopamine. One milliliter of synthetic urine was added in the quartz cuvette with the J-aggregate nanotube-integrated agarose hydrogel film, followed by the addition of DA with different concentrations in the dark. After 10 min incubation, which allowed DA to diffuse into the agarose hydrogel film and adsorb on the surface of the integrated J-aggregate nanotubes, the J-aggregate nanotube-integrated hydrogel film adhered on the wall of the quartz cuvette and was irradiated with a flashlight for 30 s and then characterized with a spectrophotometer.

ASSOCIATED CONTENT

Supporting Information

The Supporting Information is available free of charge at https://pubs.acs.org/doi/10.1021/acsomega.0c01803.

Adsorption spectra of J-aggregate nanotube-integrated agarose hydrogel films; SEM and optical microscopy images of J-aggregate nanotubes and spherulites, and chemical structures of AA and UA (PDF)

AUTHOR INFORMATION

Corresponding Author

Jiyu Fang — Advanced Materials Processing and Analysis Center and Department of Materials Science and Engineering, University of Central Florida, Orlando, Florida 32816, United States; orcid.org/0000-0002-6056-5113; Email: Jiyu.fang@ucf.edu

Authors

Nitin Ramesh Reddy — Advanced Materials Processing and Analysis Center and Department of Materials Science and Engineering, University of Central Florida, Orlando, Florida 32816, United States

Samuel Rhodes — Advanced Materials Processing and Analysis Center and Department of Materials Science and Engineering, University of Central Florida, Orlando, Florida 32816, United States

Complete contact information is available at: https://pubs.acs.org/10.1021/acsomega.0c01803

Notes

The authors declare no competing financial interest.

ACKNOWLEDGMENTS

This work was supported by the US National Science Foundation (CBET 1803690).

REFERENCES

- (1) Wise, R. A. Dopamine, learning and motivation. *Nat. Rev. Neurosci.* **2004**, *5*, 483–494.
- (2) Wiedemann, D. J.; Kawagoe, K. T.; Kennedy, R. T.; Ciolkowski, E. L.; Wightman, R. M. Strategies for low detection limit measurements with cyclic voltammetry. *Anal. Chem.* **1991**, *63*, 2965–2970.
- (3) Kim, Y. R.; Bong, S.; Kang, Y.; Yang, Y.; Mahajan, R. K.; Kim, J. S.; Kim, H. Electrochemical detection of dopamine in the presence of ascorbic acid using graphene modified electrodes. *Biosens. Bioelectron.* **2010**, 25, 2366–2369.

- (4) Kumar, A.; Selva, J. S.; Gonçalves, J. M.; Araki, K.; Bertotti, M. Nanoporous gold-based dopamine sensor with sensitivity boosted by interferant ascorbic acid. *Electrochim. Acta* **2019**, 322, No. 134772.
- (5) Xu, G.; Jarjes, Z. A.; Desprez, V.; Kilmartin, P. A.; Travas-Sejdic, J. Sensitive, selective, disposable electrochemical dopamine sensor based on PEDOT-modified laser scribed graphene. *Biosens. Bioelectron.* **2018**, *107*, 184–191.
- (6) Hsu, M. S.; Chen, Y.-L.; Lee, C.-Y.; Chiu, H.-T. Gold nanostructures on flexible substrates as electrochemical dopamine sensors. *ACS Appl. Mater. Interfaces* **2012**, *4*, 5570–5575.
- (7) Kim, J.; Jeon, M.; Paeng, K. J.; Paeng, I. R. Competitive enzymelinked immunosorbent assay for the determination of catecholamine, dopamine in serum. *Anal. Chim. Acta* **2008**, *619*, 87–93.
- (8) Fauss, D.; Motter, R.; Dofiles, L.; Rodrigues, M. A.; You, M.; Diep, L.; Yang, Y.; Seto, P.; Tanaka, K.; Baker, J.; Bergeron, M. Development of an enzyme-linked immunosorbent assay (ELISA) to measure the level of tyrosine hydroxylase protein in brain tissue from Parkinson's disease models. *J. Neurosci. Methods* **2013**, *215*, 245–257.
- (9) Park, Y. H.; Zhang, X.; Rubakhin, S. S.; Sweedler, J. V. Independent optimization of capillary electrophoresis separation and native fluorescence detection conditions for indolamine and catecholamine measurements. *Anal. Chem.* 1999, 71, 4997–5002.
- (10) Carrera, V.; Sabater, E.; Vilanova, E.; Sogorb, M. A. A simple and rapid HPLC-MS method for the simultaneous determination of epinephrine, norepinephrine, dopamine and 5-hydroxytryptamine: Application to the secretion of bovine chromaffin cell cultures. *J. Chromatogr. B* **2007**, *847*, 88–94.
- (11) Baron, R.; Zayats, M.; Willner, I. Dopamine-, L-DOPA-, adrenaline-, and noradrenaline-induced growth of Au nanoparticles: Assays for the detection of neurotransmitters and of tyrosinase activity. *Anal. Chem.* **2005**, *77*, 1566–1571.
- (12) Kong, B.; Zhu, A.; Luo, Y.; Tian, Y.; Yu, Y.; Shi, G. Sensitive and selective colorimetric visualization of cerebral dopamine based on double molecular recognition. *Angew. Chem., Int. Ed.* **2011**, *50*, 1837–1840.
- (13) Lin, Y.; Chen, C.; Wang, C.; Pu, F.; Ren, J.; Qu, X. Silver nanoprobe for sensitive and selective colorimetric detection of dopamine via robust Ag-catechol interaction. *Chem. Commun.* **2011**, 47, 1181–1183.
- (14) Mu, Q.; Xu, H.; Li, Y.; Ma, S. J.; Zhong, X. H. Adenosine capped QDs based fluorescent sensor for detection of dopamine with high selectivity and sensitivity. *Analyst* **2014**, *139*, 93–98.
- (15) Zhang, X.; Chen, X.; Kai, S.; Wang, H.-Y.; Yang, J.; Wu, F.-G.; Chen, Z. Highly Sensitive and selective detection of dopamine using one-pot synthesized highly photoluminescent silicon nanoparticles. *Anal. Chem.* **2015**, *87*, 3360–3365.
- (16) Daly, B.; Ling, J.; de Silva, A. P. Current developments in fluorescent PET (photoinduced electron transfer) sensors and switches. *Chem. Soc. Rev.* **2015**, 44, 4203–4211.
- (17) Jelley, E. E. Spectral absorption and fluorescence of dyes in the molecular state. *Nature* **1936**, *138*, 1009–1010.
- (18) Scheibe, G. Variability of the absorption spectra of some sensitizing dyes and its cause. *Angew. Chem., Int. Ed.* **1936**, 49, 563.
- (19) Nakahara, H.; Fukuda, K.; Möbius, D.; Kuhn, H. Two-dimensional arrangement of chromophores in J-aggregates of long-chain merocyanines and its effect on energy transfer in monolayer systems. *J. Phys. Chem. A* **1986**, *90*, 6144–6148.
- (20) Hestand, N. J.; Spano, F. Expanded theory of H- and J-molecular aggregates: The effects of vibronic coupling and intermolecular charge transfer. *Chem. Rev.* **2018**, *118*, 7069–7163.
- (21) Cheng, M. H. Y.; Harmatys, K. M.; Charron, D. M.; Chen, J.; Zheng, G. Stable J-aggregation of an aza-BODIPY-lipid in a liposome for optical cancer imaging. *Angew. Chem., Int. Ed.* **2019**, *131*, 13528–13523
- (22) Su, M.; Li, S.; Zhang, H.; Zhang, J.; Chen, H.; Li, C. Nano-assemblies from J-aggregated dyes: A stimuli-responsive tool applicable to living systems. J. Am. Chem. Soc. 2019, 141, 402–413.
- (23) Sun, C.; Li, B.; Zhao, M.; Wang, S.; Lei, Z.; Lu, L.; Zhang, H.; Feng, L.; Dou, C.; Yin, D.; Xu, H.; Cheng, Y.; Zhang, F. J-aggregates

- of cyanine dye for NIR-II in vivo dynamic vascular imaging beyond 1500 nm. J. Am. Chem. Soc. 2019, 141, 19221–19225.
- (24) Jones, R. M.; Lu, L.; Helgeson, R.; Bergstedt, T. S.; McBranch, D. W.; Whitten, D. G. Building highly sensitive dye assemblies for biosensing from molecular building blocks. *Proc. Natl. Acad. Sci. U.S.A.* **2001**, *98*, 14769–14772.
- (25) Ng, K. K.; Shakiba, M.; Huynh, E.; Weersink, R. A.; Roxin, A.; Wilson, B. C.; Zheng, G. Stimuli-responsive photoacoustic nanoswitch for in vivo sensing applications. *ACS Nano* **2014**, *8*, 8363–8373.
- (26) Liang, W.; He, S.; Fang, J. Y. Self-assembly of J-aggregate nanotubes and their applications for sensing dopamine. *Langmuir* **2014**, *30*, 805–811.
- (27) Deng, J.; Liang, W.; Fang, J. Y. Liquid crystal droplet embedded biopolymer hydrogel sheets for biosensor applications. *ACS Appl. Mater. Interfaces* **2016**, *8*, 3928–3932.
- (28) Hofmann, A. F.; Rods, A. Physicochemical properties of bile acids and their relationship to biological properties: An overview of the problem. *J. Lipid Res.* **1984**, 25, 1477–1489.
- (29) Rhodes, S.; Liang, W.; Shteinberg, E.; Fang, J. Y. Formation of spherulitic J-aggregate spherulites from the co-assembly of lithocholic acid and cyanine dye. *J. Phys. Chem. Lett.* **2017**, *8*, 4504–4509.
- (30) Terech, P.; Jean, B.; Ne, F. Hexagonally ordered ammonium lithocholate self-assembled nanotubes with highly monodisperse solution. *Adv. Mater.* **2006**, *18*, 1571–1574.
- (31) Ju, C.; Bohne, C. Dynamics of probe complexation to bile salt aggregates. J. Phys. Chem. B 1996, 100, 3847–3854.
- (32) Cao, Z.; Gilbert, R. J.; He, W. Simple agarose—chitosan gel composite system for enhanced neuronal growth in three dimensions. *Biomacromolecules* **2009**, *10*, 2954—2959.
- (33) Dillon, G. P.; Yu, X.; Sridharan, A.; Ranieri, J. P.; Bellamkonda, R. V. The influence of physical structure and charge on neurite extension in a 3D hydrogel scaffold. *J. Biomater. Sci., Polym. Ed.* **1998**, 9, 1049–1069.
- (34) Marc, D. T.; Ailts, J. W.; Ailts-Campeau, D. C.; Bull, M. J.; Olson, K. Neurotransmitters excreted in the urine as biomarkers of nervous system activity: validity and clinical applicability. *Neurosci. Biobehav. Rev.* **2011**, *35*, 635–644.
- (35) Knoester, J.; Agranovich, V. M. Electronic Excitations in Organic Based Nanostructures; Agranovich, V. M.; Bassani, G. F., Eds.; Thin Films and Nanostructures; Elsevier: Amsterdam, Oxford, 2003; Vol. 31.
- (36) Klegeris, A.; Korkina, L. G.; Greenfield, S. A. Autoxidation of dopamine: A comparison of luminescent and spectrophotometric detection in basic solutions. *Free Radical Biol. Med.* **1995**, *18*, 215–222
- (37) García-Moreno, M.; Rodríguez-López, J. N.; Martínez-Ortiz, F.; Tudela, J.; Varón, R.; García-Cánovas, F. Effect of pH on the oxidation pathway of dopamine catalyzed by tyrosinase. *Arch. Biochem. Biophys.* **1991**, 288, 427–434.
- (38) Young, T. E.; Babbitt, B. W. Electrochemical study of the oxidation of alpha.-methyldopamine, alpha.-methylnoradrenaline, and dopamine. *J. Org. Chem.* **1983**, *48*, 562–566.
- (39) Mohammad-Shiri, H.; Ghaemi, M.; Riahi, S.; Akbari-Sehat, A. Computational and electrochemical studies on the redox reaction of dopamine in aqueous solution. *Int. J. Electrochem. Sci.* **2011**, *6*, 317–326
- (40) Bredas, J. L.; Silbey, R.; Boudreux, D. S.; Chance, R. R. Chainlength dependence of electronic and electrochemical properties of conjugated systems: Polyacetylene, polyphenylene, polythiophene, and polypyrrole. *J. Am. Chem. Soc.* **1983**, *105*, 6555–6559.
- (41) Howell, R. R.; Wyngaar, J. B. On the mechanism of peroxidation of uric acid by hemoproteins. *J. Biol. Chem.* **1960**, 226, 3544–3550.